PHYSICAL REVIEW D

PARTICLES AND FIELDS

THIRD SERIES, VOLUME 24, NUMBER 11 1 DECEMBER 1981

Strange-particle production from neutrino interactions in the BNL 7-foot bubble chamber

N. J. Baker, P. L. Connolly, S. A. Kahn, H. G. Kirk, M. J. Murtagh, R. B. Palmer, N. P. Samios, and M. Tanaka

Brookhaven National Laboratory, Upton, New York 11973

(Received 8 July 1981)

Strange-particle production in charged-current and neutral-current neutrino interactions has been studied using the BNL 7-foot deuterium bubble chamber. A total of 37 charged-current and 9 neutral-current events in the data sample contain one or more strange particles. Three events have $\Delta S \neq 0$. The measured total rate for neutral V^0 production in charged-current interactions is $(4.2 \pm 1.0)\%$. Cross sections are given for low-multiplicity reactions involving neutral strange particles.

I. INTRODUCTION

Strange-particle production in neutrino interactions is in principle well described by the Glashow-Iliopoulos-Maiani (GIM) mechanism.[1] Associated strangeness production ($\Delta S = 0$) and strangeness-changing transitions of the type $\Delta S = \Delta Q$ (ΔQ is the change in charge of the baryon system from initial to final state) are allowed. Although transitions of the type $\Delta S = -\Delta Q$ are forbidden, when a charm particle is produced its decay to a strange particle produces an apparent $\Delta S = -\Delta Q$ transition. In practice few experiments can isolate the different classes of strangeness production and thus little detailed information has been obtained to date. All the present data come from bubble-chamber experiments where neutral-strange-particle decays ($K_S \to \pi^+\pi^-$, $\Lambda \to p\pi^-$) are easily observed. However, in these experiments it is very difficult to identify charge kaons and hyperons by their decays or to separate kaons from pions by ionization.

We report here on an experiment to study strange particle production near threshold in neutrino interactions in a light liquid. In this energy region the particle momenta are usually low and this, coupled with a light target, allows the use of kinematic constraints to identify charged kaons. A total of 37 charged-current and 9 neutral-current events were found in a 1 000 000 (200 000) picture neutrino exposure of the BNL 7-foot bubble chamber filled with deuterium (hydrogen) liquid. Previous results from this experiment reporting events where $\Delta S \neq 0$ have been published.[2,3] This paper presents the results of the analysis of the complete strange-particle sample. The contents of this paper include a review of the $\Delta S \neq 0$ events, inclusive strange-particle production rates and distributions, a discussion of neutral-current strangeness production, and the study of exclusive strange-particle final states.

Two other experiments have published results on strange-particle production near threshold. The ANL 12-foot chamber experiment[4] was a deuterium experiment. However, the neutrino flux peaks significantly lower than that in the present experiment. Consequently the statistics are smaller and the probability for charm production is negligible. The Gargamelle bubble-chamber experiment in the CERN Proton Synchrotron neutrino beam[5] is a relatively-high-statistics experiment. However, it uses a heavy liquid as the target. Consequently, one cannot use kinematic constraints to identify charged strange particles and large nuclear-correction effects must be taken into account in the statistical calculations for the various strange-particle production mechanisms.

II. EXPERIMENTAL PROCEDURE

The results presented here come from an exposure of the BNL 7-foot bubble chamber filled with deuterium (hydrogen) in the Alternating Gradient Synchrotron (AGS) broad-band neutrino beam.[6] The neutrino energy spectrum peaks at about 1.0 GeV with 33% of the events above the threshold for strange-particle production (Fig. 1). The 7-foot bubble chamber operates in a 25-kG magnetic

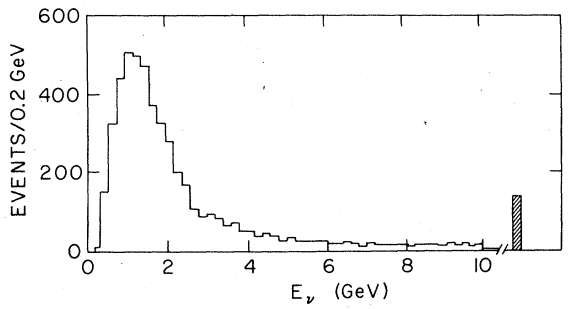

FIG. 1. Distribution of the calculated neutrino energy E_ν for the charged-current events.

field and has an internal volume of 10 m³. Four 2-in.-thick stainless-steel plates were inserted into the bubble chamber to provide muon identification and to aid in the selection of neutral-current events. The film was scanned for events containing at least two charged tracks at the primary vertex or at least one charged track at the primary vertex and one or more V^0's (neutral strange particles). The total event sample contains 5000 (385) charged current events in the D_2 (H_2) exposure.

The background from incoming charged particles was removed by requiring that the total visible momentum $|\vec{P}_{vis}|$ be greater than 300 MeV/c and that the angle between $\vec{P}_{vis}$ and the beam direction be less than 50°. Approximately a quarter of the film was rescanned, yielding a single-scan efficiency of 94% for finding events containing at least one V^0. All events were measured, reconstructed, and kinematically fitted to appropriate reaction interpretations. Each event was then reviewed by a physicist to check the results of the measurement and where possible to identify the particles using ionization information. The V^0 events were separated into charged-current and neutral-current samples on the basis of the existence of a muon candidate. A muon candidate is defined to be a negative track that leaves the chamber without interacting, stops in the plates with a range consistent with a muon interpretation, or decays into an electron. Although most charged-current events have a single muon candidate, when an ambiguity exists the candidate with the largest transverse momentum with respect to the hadron direction is selected. Charged-hadron ambiguities are resolved if possible using ionization information and kinematic fitting. The remaining hadron ambiguities are left unresolved. This has an effect on the calculation of neutrino energy that we will discuss later. The V^0 data sample contains 37 charged-current events and 9 neutral-current events (Tables I and II). For 23 of the 24 charged-current events that have no missing neutrals, an unambiguous choice can be made for the V^0 using the three-constraint production fit. As the remaining ambiguous event could be interpreted as

TABLE I. Topologies of the 37 charged-current events with strangeness.

Reaction	Observed Events	ΔS	Number of constraints
$\nu n \to \mu^- p \pi^+ \pi^- \bar{K}^0$	1	−1	3
$\nu n \to \mu^- K^+ \Lambda$	11	0	3
$\nu n \to \mu^- \pi^+ K^0 \Lambda$	1	0	3
$\nu n \to \mu^- \pi^- \pi^+ K^+ \Lambda$	1	0	3
$\nu n \to \mu^- \pi^- K^+ \Sigma^+$	1	0	3
$\nu n \to \mu^- h^+ K^0 X^0$	2	0	0
$\nu n \to \mu^- h^- h^+ h^+ K^0 X$	3	0	0
$\nu n \to \mu^- h^+ \Lambda X^0$	3	0	0
$\nu n \to \mu^- \pi^+ K^0 \Lambda X$	1	0	0
$\nu p \to \mu^- \pi^- \pi^+ \pi^+ \pi^+ \Lambda$	1	−1	3
$\nu p \to \mu^- p \pi^+ K^0$	1	+1	3
$\nu p \to \mu^- \pi^+ K^+ \Lambda$	$4\frac{1}{2}$	0	3
$\nu p \to \mu^- h^- h^- h^+ h^+ \pi^+ K^0$	1	0	3
$\nu p \to \mu^- K^0 K^+ p$	$\frac{1}{2}$	0	3
$\nu p \to \mu^- h^+ h^+ K^0 X$	1	0	0
$\nu p \to \mu^- h^+ \pi^+ \Lambda X$	3	0	0
$\nu p \to \mu^- \pi^+ \pi^+ \Lambda K^0 X$	1	0	0

TABLE II. Topologies of the 9 neutral-current events with strange particles produced.

Reaction	Observed events
$\nu n \to \nu h^+ h^- K^0$	2
$\nu p \to \nu h^+ \Lambda$	3
$\nu p \to \nu \pi^+ \Lambda$ [a]	1
$\nu p \to \nu K^0 \Lambda \pi^+$	1
$\nu p \to \nu h^+ \pi^+ \pi^- \Lambda$	1
$\nu p \to \nu h^+ K^0 \pi^0$ [b]	1

[a] This event, which has a positive track that is overstopped as K^+ event, is most likely $\nu p \to \nu K^0 \Lambda \pi^+$.
[b] Photon from π^0 is visible.

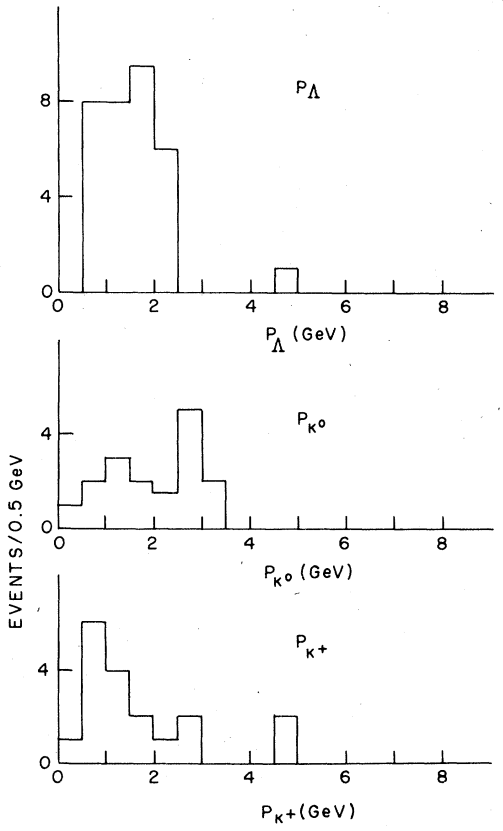

FIG. 2. Momentum distribution of (a) Λ, (b) K^0_S, and (c) K^+. The K^+'s are identified by constrained kinematic fits at the production vertex.

either $\mu^- K^0 K^+ p$ or $\mu^- K^+ \pi^+ \Lambda$, it is assigned to both categories with a weight of $\frac{1}{2}$. Only two V^0's in the sample of events with missing neutrals had ambiguous interpretations. In these events the Λ interpretation was chosen over the K_S.[7] Figure 2 shows the momentum distribution of the K_S, Λ, and K^+ produced in the neutrino events. The K^+'s are identified in the three-constraint production fits. The K^0 momentum distribution is important for the discussion of backgrounds in the neutral-current channels.

III. SINGLE-STRANGE-PARTICLE PRODUCTION

Three of the charged-current events are not consistent with being associated strange-particle production. In a light liquid at the energies encountered in this experiment the kinematic-fitting process distinguishes very well between different hypotheses. For example, Fig. 3 shows the longitudinal constraint

$$C_{\parallel} = \sum (E_i - P_{\parallel i}) - M_T$$

(E_i is the energy, $P_{\parallel i}$ the momentum in the beam direction for an individual charged secondary particle, and M_T is the mass of the target), for the $\Delta S = 0$ events, $\Delta S \neq 0$ events, and a control sample without strange particles. Since the neutrino has no mass, $C_{\parallel} = 0$ (within errors) if there are no missing neutral particles. When there are missing neutrals $C_{\parallel} < 0$. The region $C_{\parallel} > 0$ (outside of errors) is unphysical for neutrino interactions. However, if light particles in the final state are incorrectly identified as heavier particles (e.g., π^+ as a K^+), then events will appear in the $C_{\parallel} > 0$ region. The three $\Delta S \neq 0$ events when interpreted as associated production are shown as unshaded in Fig. 3(a).[8] When interpreted as $\Delta S \neq 0$, $C_{\parallel}$ is consistent with zero as shown in Fig. 3(b).

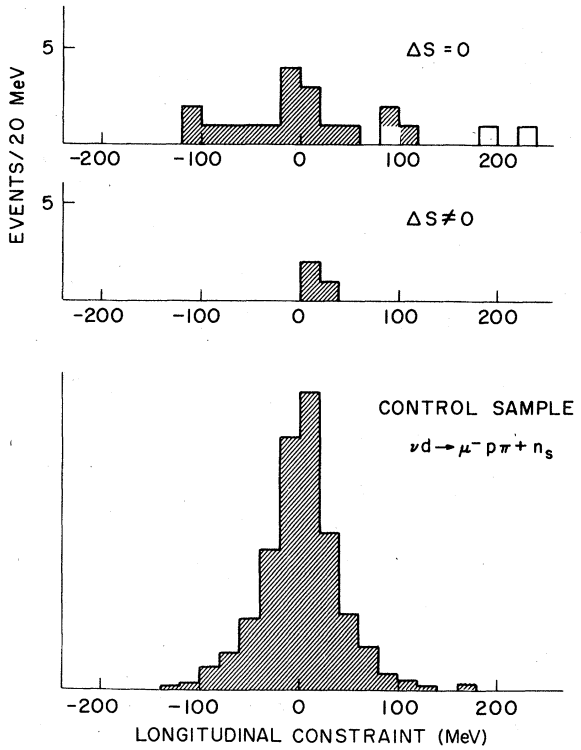

FIG. 3. Distribution of the longitudinal constraint $C_{\parallel}$ for (a) $\Delta S = 0$, (b) $\Delta S \neq 0$, and (c) $\nu d \to \mu^- p \pi^+ n_s$ events used as a control sample. The $\Delta S \neq 0$ events in (b) are shown in (a) as unshaded when interpreted as normal $\Delta S = 0$ events.

From Table I it is clear that production of strange particles in neutrino interactions is dominated by $\Delta S = 0$ processes where the total strangeness in the final state is equal to zero (the total strangeness of the initial state). The rarer $\Delta S \neq 0$ processes can also occur in neutrino interactions. The $\Delta S = -1$ process is forbidden unless associated with the decay of charm. It can only occur above the threshold for charm production (only 14% of the events are above this threshold) and is expected to be suppressed by $\sin^2\theta_C$. The $\Delta S = 1$ process is allowed if a $\bar{u}$ or s quark from the sea is struck. This process is expected to be smaller than charm production since it is suppressed both by $\sin^2\theta_C$ and by the probability for finding the $\bar{u}$ or s quark. However, since the energy threshold for this $\Delta S = +1$ process is lower than the threshold for associated production or charm production, more flux is available to this reaction (an order of magnitude more than for charm) and one might expect the rate to be comparable to charm.

One of the three $\Delta S \neq 0$ events was published[1] as the first example of a charmed baryon, the reaction being

$$\nu p \to \mu^- \Sigma_c^{++}(2426)$$
$$\Sigma_c^{++}(2426) \to \Lambda_c^+(2260)\pi^+$$
$$\Lambda_c^+(2260) \to \Lambda\pi^+\pi^+\pi^- .$$

The Λ_c^+ mass and the $\Sigma_c^{++} - \Lambda_c^+$ mass difference in this event were found to be 2260 ± 20 MeV (Ref. 9) and 166 ± 3 MeV, respectively. A second charm event[2] that was found decayed through the kaonic mode.

$$\nu n \to \mu^- \Lambda_c^+$$
$$\Lambda_c^+ \to K^{*-}(890) p \pi^+$$
$$K^{*-}(890) \to K^0 \pi^- .$$

The third event, corresponding to the reaction $\nu p \to \mu^- K_S \pi^+ p$, is interpreted as single strangeness

TABLE III. Summary of properties of $\Delta S \neq 0$ events.

Reaction	ΔS	E_ν (GeV)	x	y	W (GeV)	$M_{\Lambda_c^+}$ (GeV)
$\nu p \to \mu^- \Lambda \pi^+ \pi^+ \pi^+ \pi^-$	−1	13.5	0.31	0.28	2.426	2.260
$\nu n \to \mu^- p \pi^+ \pi^- \bar{K}^0$	−1	3.9	0.23	0.74	2.254	2.254
$\nu p \to \mu^- p \pi^+ K^0$	+1	5.2	0.11	0.39	2.059	
$\nu n \to \mu^- \Lambda \pi^+ \pi^+ \pi^-$	a	9.0	0.50	0.69	2.271	2.271

[a]The fourth event can also be interpreted as $\nu n \to \mu^- \Lambda K^+ \pi^+ \pi^-$. It is included in this table for comparison.

production off the quark sea. The $K_S^0 \pi^+$ effective mass is in the vicinity of the $K^*(890)$ suggesting $\Delta S = +1$ for this event. The scaling variable $x = Q^2/[2m_p(E_\nu - E_\mu)]$ is 0.11, favoring the interpretation of sea production for this event. A fourth candidate for $\Delta S \neq 0$ was found. This event, although consistent with quasielastic production of Λ_c^+ decaying to $\Lambda \pi^+ \pi^+ \pi^-$ with $M_{\Lambda_c^+} = 2271 \pm 13$ MeV, could be interpreted equally well as $\nu p \to \mu^- \Lambda K^+ \pi^+ \pi^-$ since the momentum of a positive track is too fast to distinguish between K^+ and π^+ hypotheses. The $\Delta S = 0$ interpretation will be used for the rest of this paper. Table III summarizes the properties of the $\Delta S \neq 0$ events. The ambiguous candidate is included for comparison. Correcting for the V^0 detection efficiency the production rate for charmed baryons, where the charmed-particle decays into only a V^0 and charged tracks, relative to the rate for charged-current events above the effective charm threshold,[10] is $(1.0 \pm 0.7)\%$. The total charm-production rate includes modes that produce π^0's and/or a neutron to which this experiment is not sensitive. Correcting for these neutral decays yields a total rate at the level of ~3–5%, which is compatible with the expected Cabibbo rate in the GIM model.

IV. ASSOCIATED STRANGE-PARTICLE PRODUCTION

The rate for total neutral-strange-particle production in charged-current events is determined in a fiducial volume where the event normalization is well understood. Seventy-two percent of the charged-current V^0 events are within this volume. The following corrections have been made in the calculation of this rate.

(1). Losses from V^0 scanning inefficiencies ($\epsilon_{scan} \sim 0.95$).

(2). Losses of K_S's or Λ's that decay too close to the origin to be distinguished. A cut is made for V^0's closer than 1 cm to the origin where the detection efficiency is poor. Using the K_S^0 and Λ lifetimes we calculate that this cut removes 12% of the events.

(3). Losses of K_S's or Λ's that leave the chamber or hit the plates before they have a chance to decay (~5%).

(4). Corrections for V^0's that decay into unseen modes (such as $K_S \to \pi^0 \pi^0$, K_L, $\Lambda \to n\pi^0$, etc.).

The overall efficiency for seeing a K^0 (Λ) is $\epsilon_{K^0} = 0.26$ ($\epsilon_\Lambda = 0.53$). Table IV shows the raw and corrected numbers for single-K^0, single-Λ, K^0K^0, and $K^0\Lambda$ events. The corrected single-K^0 (single-Λ) events are mainly the $K^0K^\pm$ ($K^+\Lambda$) channels but the $\Delta S \neq 0$ events are included in these numbers. Normalizing to the number of charged-current events above the threshold for strangeness production ($W > 1.6$ GeV, $E_\nu > 1.5$ GeV) we find

$$\frac{\sigma(\nu d \to \mu^- V^0 \cdots)}{\sigma(\nu d \to \mu^- \cdots)} = (4.2 \pm 1.0)\%,$$

$$\frac{\sigma(\nu d \to \mu^- K^0 \cdots)}{\sigma(\nu d \to \mu^- \cdots)} = (2.4 \pm 0.9)\%,$$

TABLE IV. Raw and corrected number of strange-particle events.

	Charged current		Neutral current	
	Raw events	Corrected events	Raw events	Corrected events
Single K_0	9.5	24.9 ± 3.6	3	7.7 ± 7.0
Single Λ	23.5	31.9 ± 6.8	5	5.1 ± 6.5
K^0K^0	0	0	0	0
$K^0\Lambda$	3	20.3 ± 11.7	1	6.8 ± 6.8
Total	36	77.1 ± 14.0	9	19.6 ± 11.7
Estimated background	1	2 ± 2	1.5	3.3 ± 3.0

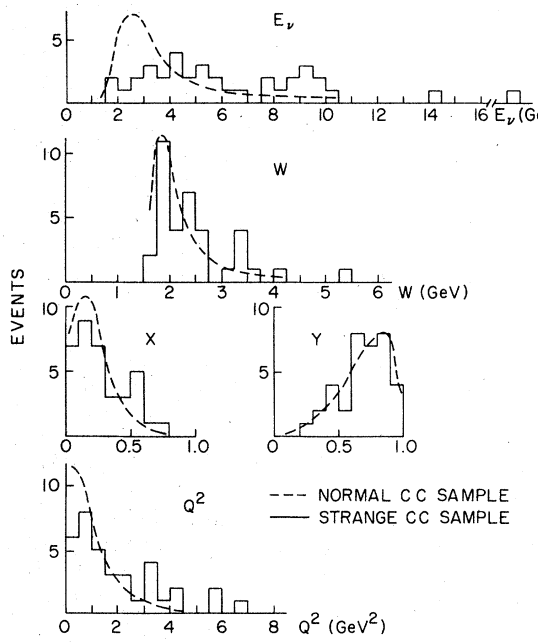

FIG. 4. The neutrino variables E_ν, W, x, y, and Q^2 for the neutral-strange-particle charged-current sample. Similar distributions for the normal charged-current sample with $E_\nu > 1.5$ GeV and $W > 1.6$ GeV are shown as a dashed line.

$$\frac{\sigma(\nu d \to \mu^- \Lambda \cdots)}{\sigma(\nu d \to \mu^- \cdots)} = (2.8 \pm 1.0)\% .$$

The rate for V^0 production counts events that contain more than one V^0 only once, so this rate is less than the sum of the K^0 and Λ rates. The CERN-PS Gargamelle experiment[11] measures a total strange-particle charged-current rate of $(8 \pm 2)\%$. The ANL 12-foot bubble-chamber experiment[12] gives a rate of $(3.4 \pm 1.3)\%$ for visible neutral-strange-particle production. Both of these measurements are consistent with the result obtained here.

In Figs. 4(a)–4(e) the E_ν, W, x, y, and Q^2 distributions are presented for the sample of charged-current events containing at least one V^0. Q^2 is the negative of the square of the four-momentum transfer from the neutrino to the muon, $W \equiv [m_p^2 - 2m_p(E_\nu - E_\mu) - Q^2]^{1/2}$ is the total hadronic mass, $x = Q^2/2m_p(E_\nu - E_\mu)$, and $y = (E_\nu - E_\mu)/E_\nu$. The neutrino energy used in these calculations is estimated in the following manner: The fitted energy is used when there is a constrained fit. When particles are missing, the neutrino energy is estimated by using the average of the minimum energy obtained assuming a missing strange-particle topology and the minimum energy obtained assuming a missing-nonstrange-particle topology. The superimposed curves in Fig. 4 are the same distributions for the total charged-current (TCC) sample with the cuts, $E_\nu > 1.5$ GeV and $W > 1.6$ GeV, to simulate the strange-particle threshold.[13] Figure 4(a) implies that strange-particle production is small near threshold and rises rapidly with energy. The x and y distributions are similar for the strange-particle charged-current (SCC) sample and the TCC sample. This is expected because both associated strange-particle production and normal charged-current processes are dominated by production off the valence quark. The absence of events at low y is a kinematic effect due to the strange-particle-mass threshold. Figure 5 shows the rate for visible V^0 production as a function of W. Also shown are similar results for the ANL 12-foot bubble-chamber experiment[4] and a Fermilab 15-foot bubble-chamber experiment.[14] The agreement between experiments is good.

In deuterium one can separate interactions involving a proton target from those involving a neutron target on the basis of charge multiplicity. Figures 6(a)–6(d) show the E_ν and W distributions for events off neutrons and protons separately. Because the reaction $\nu n \to \mu^- K^+ \Lambda$ has the lowest threshold, we expect neutron-target events to start at a lower energy. All of the V^0 events produced on neutrons with $E_\nu < 4$ GeV correspond to the reaction $\nu n \to \mu^- K^+ \Lambda$.

The nine events with V^0's that do not have a muon candidate are interpreted as neutral-current events. Table II lists the topologies of the events.

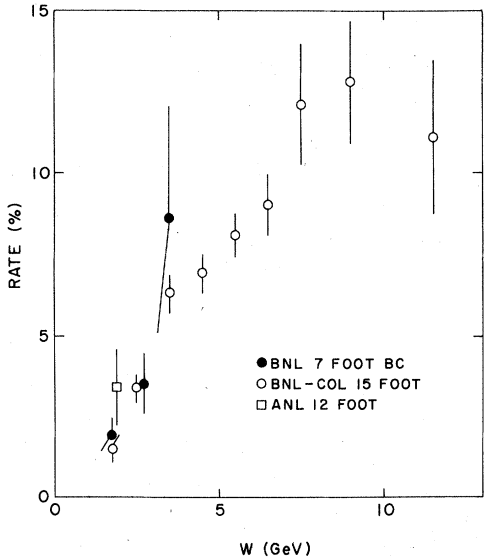

FIG. 5. Rate for visible strangeness production as a function of the hadronic invariant mass W. Results from the ANL experiment (Ref. 2) and the BNL-Columbia experiment in the Fermilab 15-foot bubble chamber are presented for comparison (Ref. 12).

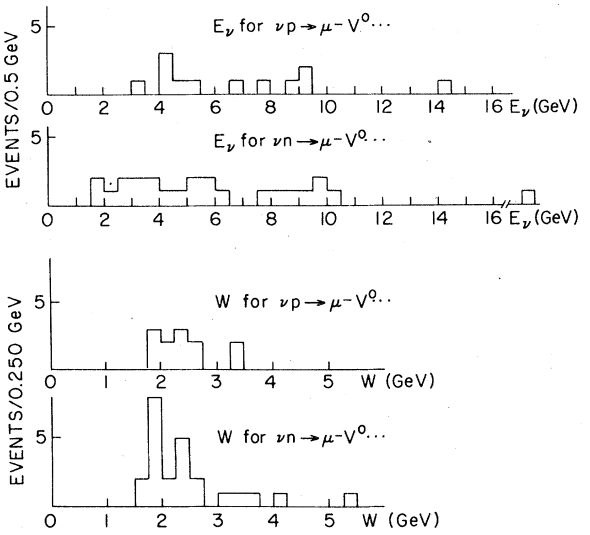

FIG. 6. E_ν and W distributions for reactions on protons, (a) and (c), and on neutrons, (b) and (d), are shown.

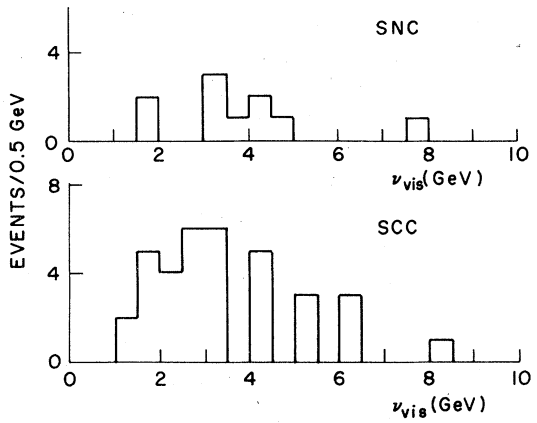

FIG. 7. The visible hadronic energy ν_{vis} for (a) the strange-particle neutral-current events and (b) strange-particle charged-current events.

It is not possible to say if there are missing neutral hadrons in any of these reactions since there is always a missing neutrino. Possible backgrounds in the strange-particle neutral-current sample (SNC) from neutron, K_L, and $\bar{\nu}$ sources have been investigated. The neutron flux has been obtained from a scan for events corresponding to the reaction $np \to pp\pi^-$. Fourteen events with one-constraint fits for this reaction were found. From the incident neutron momentum distribution obtained from the $np \to pp\pi^-$ events, the neutron flux is found to be negligible above the strange-particle threshold. The $\bar{\nu}$-induced background is expected to be small.[15] The largest background comes from K_L interactions. The source of this background is neutrino interactions producing K_L's upstream of the bubble chamber. From the observation of K_S produced by neutrino interactions inside the bubble chamber, the estimated K_L flux is 45 ± 30 particles. Using the momentum distribution of the K_S's (Fig. 2) and K^0 reaction cross sections, we estimate the K_L background to be 1.3 ± 1.0 events. As a check on the validity of the background estimates, the visible hadronic energy of the SNC events is shown in Fig. 7. The SCC visible hadronic energy is shown for comparison. The SNC hadronic-energy spectrum is higher than would be expected from the momentum distributions of the K_L^0 of n background events. The total background in the neutral-current events is 1.5 ± 1.2 events. There is a loss of 0.5 SNC events which have a negative hadron which is interpreted as a fake μ^-. The relative rate of strangeness-producing neutral-current to strangeness-producing charged-current interactions is

$$\frac{\sigma(\nu d \to \nu V^0 \cdots)}{\sigma(\nu d \to \mu^- V^0 \cdots)} = 0.22 \pm 0.14 ,$$

where V^0 represents K^0 or Λ corrected for missing-neutral modes. Gargamelle has reported a ratio[5] of $0.34^{+0.17}_{-0.09}$ for strange-particle neutral-current events to strange-particle charged-current events. Since the Gargamelle ratio includes both charged and neutral strange particles, it cannot be directly compared to our result.

V. EXCLUSIVE STRANGE-PARTICLE FINAL STATES

At BNL energies ν interactions are dominated by a few low-multiplicity final states. Table V shows the raw and corrected (for the above-mentioned

TABLE V. Flux-averaged cross section for low-multiplicity exclusive reactions.

Reaction	Events in fiducial volume $1.5 < E_\nu < 6$ GeV	$\langle E_\nu \rangle$ (GeV)	Corrected events	Flux-averaged cross section (10^{-40} cm^2)	Number of constraints in fit
$\nu n \to \mu^- K^+ \Lambda$	8	3.6	16.6	4.0 ± 1.4	3
$\nu p \to \mu^- K^+ \pi^+ \Lambda$	2	3.8	3.9	0.9 ± 0.7	3
$\nu n \to \mu^- K^0 \pi^+ \Lambda$	1	5.5	3.4	0.8 ± 0.8	3
$\nu p \to \nu K^+ \Lambda$	2	2.8	3.8	0.9 ± 0.6	0

TABLE VI. Cross section for $\nu n \to \mu^- K^+ \Lambda$ for different energies.

E_ν (GeV)	Events in fiducial volume	Cross section (10^{-40} cm^2)	Theoretical cross section (10^{-40} cm^2)
1.5–3.0	3	1.7 ± 1.0	0.6
3.0–4.5	3	15 ± 8	2.7
4.5–6.0	2	33 ± 24	4.8
1.5–6.0	8	4.0 ± 1.4	0.93

V^0 efficiencies) number of events in various exclusive channels. The cross sections listed are normalized to the quasielastic channel[6] $\nu n \to \mu^- p$, where the cross section can be calculated theoretically. The listed cross sections are averaged over the flux between 1.5 and 6.0 GeV. The mean energy of the ν flux in this region is 1.8 GeV. However, the mean energy of the observed events in the channels listed in Table V are higher, indicating that these cross sections are rapidly growing in the energy range accessible to this experiment. Since there are no kinematic constraints for the neutral-current channels, these channels may include missing hadronic neutrals.

It is interesting to compare our cross section for $\nu n \to \mu^- K^+ \Lambda$ with a theoretical calculation[16] for the reaction based on the BORN approximation. We have integrated the theoretical cross section over the flux obtained from the quasielastic events.

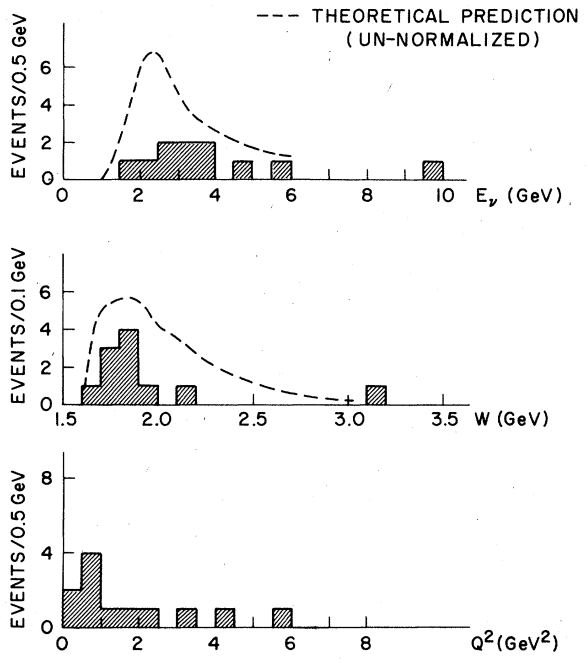

FIG. 8. E_ν, W, and Q^2 distributions for the reaction $\nu n \to \mu^- K^+ \Lambda$. The superimposed curve gives the (unnormalized) form of the distribution expected from integrating the Shrock results with the BNL flux.

Table VI gives our experimental cross section and the theoretical cross section in three energy bins along with the overall average. The experimental cross section is ~4 times as large as the cross section predicted by Shrock.[17] This is similar to the results on $\nu n \to \mu^- K^+ \Lambda$ from the ANL 12-foot bubble-chamber experiment. Figures 8(a)–8(c) show the distributions of E_ν, W, and Q^2 for the $\mu^- K^+ \Lambda$ events. The superimposed curve is that obtained from the Born approximation with arbitrary normalization. Although the statistics are small, the events fall off in W faster than the calculated curve implies. Assuming that the fraction of $K^+ \Lambda$ events with undetected missing neutral hadrons in the final state is the same for neutral-current events as for charged-current events, one can calculate the ratio for the reaction $\nu p \to \nu K^+ \Lambda$ to $\nu n \to \mu^- K^+ \Lambda$:

$$R^+ = \frac{\sigma(\nu K^+ \Lambda)}{\sigma(\mu^- K^+ \Lambda) + \sigma(\mu^- K^+ \Lambda X^0)} = 0.18 \pm 0.13 ,$$

where X^0 represents undetected neutrals. This result is consistent with the Shrock model.

No events for the reaction $\nu n \to \nu K^0 \Lambda$ were found in our data sample. Such an event would appear

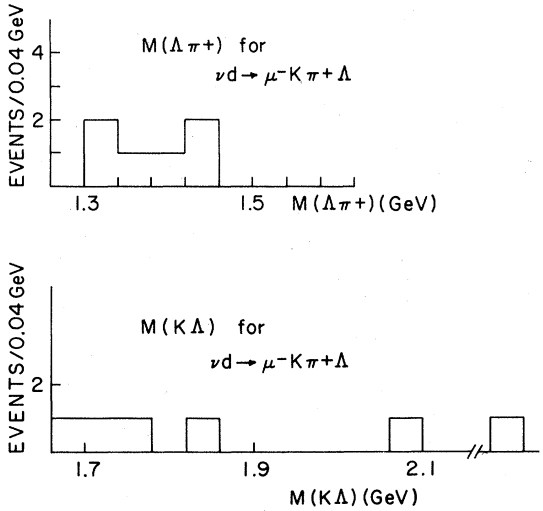

FIG. 9. (a) $\Lambda \pi^+$, and (b) $K \Lambda$ masses from $\nu d \to K \pi^+ \Lambda$ events.

as two V^0's pointing to a common origin where there are no visible charged tracks. We find that the 90% c.l. upper limit for such an interaction is

$$R^0 = \frac{\sigma(\nu K^0 \Lambda)}{\sigma(\mu^- K^+ \Lambda) + \sigma(\mu^- K^+ \Lambda X^0)} < 0.20 .$$

The $\mu^- K^+ \pi^+ \Lambda$ and $\mu^- K^0 \pi^+ \Lambda$ events were examined for evidence of resonance structure in the $\Lambda\pi^+$ of $K^{+(0)}\Lambda$ masses. Figure 9 shows the $\Lambda\pi^+$ and $K^{+(0)}\Lambda$ masses for these events. All of these events have the $\Lambda\pi^+$ mass between 1.300 and 1.45 GeV, although the distribution about the $Y^*(1385)$ mass is broader than the resonance width.

VI. CONCLUSION

In this experiment all three mechanisms for strange-particle production present in the GIM model have been observed. The number of charm and $\Delta S = \Delta Q$ events observed while consistent with the model are too few to yield a good measurement of their respective rates. The measurement of associated production is consistent both with other measurements near threshold and with higher-energy results. At the energies available in this experiment a few exclusive channels dominate the strange-particle production. The number of events observed in the channel $\nu n \to \mu^- K^+ \Lambda$ is not consistent with present theoretical calculations.

We have observed neutral-current strange-particle events. The rate of production is consistent with that reported by the Gargamelle collaboration.

ACKNOWLEDGMENTS

We would like to thank the AGS and 7-foot bubble-chamber staff, our scanning staff, and Fern Coyle, who helped in editing the data, for their efforts that made this experiment possible. This work was supported by the U. S. Department of Energy under Contract No. DE-AC02-76CH00016.

[1]S. L. Glashow, J. Iliopoulos, and L. Maiani, Phys. Rev. D 2, 1285 (1970).
[2]E. G. Cazzoli *et al.*, Phys. Rev. Lett. 34, 1125 (1975).
[3]A. M. Cnops *et al.*, Phys. Rev. Lett. 42, 197 (1979).
[4]S. J. Barish *et al.*, Phys. Rev. Lett. 33, 1446 (1974); Phys. Rev. D 19, 2521 (1979).
[5]H. Deden *et al.*, Phys. Lett. 58B, 361 (1975).
[6]N. J. Baker *et al.*, Phys. Rev. D 23, 2499 (1981).
[7]The Λ interpretation is chosen over the K_S interpretation since the kinematic region for a K_S/Λ ambiguity is a large fraction of the Λ-decay phase space and a small fraction of the K_S-decay phase space.
[8]The second event does have a lower probability fit for a $\Delta S = 0$ interpretation; however, the charm interpretation is favored as discussed in Ref. 3.
[9]The errors quoted here have been revised since the original publication.
[10]We have assumed the threshold behavior predicted by R. Shrock and B. W. Lee, Phys. Rev. D 13, 2539 (1976).
[11]The Gargamelle calculations are for $E_\nu > 1.0$ GeV and $W > 1.6$ GeV. From the numbers in their publication (Ref. 3), we have estimated the rate for V^0 production to be $(5.7 \pm 1)\%$.
[12]The ANL calculations (Ref. 4) are for $E_\nu > 1.5$ GeV and $1.4 \leq W \leq 3.0$ GeV. If we assume similar V^0 detection efficiencies to those in this experiment the rate for V^0 production would be ~6%.
[13]The neutrino energy for the TCC sample is the minimum energy obtained assuming a nonstrange topology.
[14]C. Baltay, private communication.
[15]W. Lee *et al.*, Phys. Rev. Lett. 38, 202 (1977).
[16]R. Shrock, Phys. Rev. D 12, 2049 (1975).
[17]Although the Born approximation breaks down at high E_ν and large W, it should overestimate the cross section.